

REPORT DOCUMENTATION PAGE

Form Approved
OMB No. 0704-0188

Public reporting burden for this collection of information is estimated to average 1 hour per response, including the time for reviewing instructions, searching existing data sources, gathering and maintaining the data needed, and completing and reviewing this collection of information. Send comments regarding this burden estimate or any other aspect of this collection of information, including suggestions for reducing this burden to Department of Defense, Washington Headquarters Services, Directorate for Information Operations and Reports (0704-0188), 1215 Jefferson Davis Highway, Suite 1204, Arlington, VA 22202-4302. Respondents should be aware that notwithstanding any other provision of law, no person shall be subject to any penalty for failing to comply with a collection of information if it does not display a currently valid OMB control number. **PLEASE DO NOT RETURN YOUR FORM TO THE ABOVE ADDRESS.**

1. REPORT DATE October 2014		2. REPORT TYPE Annual		3. DATES COVERED 30 SEP 2013 – 29 SEP 2014	
4. TITLE AND SUBTITLE Targeting Phosphatidylserine for Radioimmunotherapy of Breast Cancer Brain Metastasis				5a. CONTRACT NUMBER	
				5b. GRANT NUMBER W81XWH-12-1-0317	
				5c. PROGRAM ELEMENT NUMBER	
6. AUTHOR(S) Dawen Zhao, M.D., Ph.D. Email: dawen.zhao@utsouthwestern.edu				5d. PROJECT NUMBER	
				5e. TASK NUMBER	
				5f. WORK UNIT NUMBER	
7. PERFORMING ORGANIZATION NAME(S) AND ADDRESS(ES) University of Texas Southwestern Medical Center at Dallas Dallas, TX 75390				8. PERFORMING ORGANIZATION REPORT NUMBER	
9. SPONSORING / MONITORING AGENCY NAME(S) AND ADDRESS(ES) U.S. Army Medical Research and Materiel Command Fort Detrick, Maryland 21702-5012				10. SPONSOR/MONITOR'S ACRONYM(S)	
				11. SPONSOR/MONITOR'S REPORT NUMBER(S)	
12. DISTRIBUTION / AVAILABILITY STATEMENT Approved for Public Release; Distribution Unlimited					
13. SUPPLEMENTARY NOTES					
14. ABSTRACT Brain metastasis occurs in ~30% of metastatic breast cancer patients. The prognosis is extremely poor, with a median survival of 4-6 months even with aggressive treatment. Thus, there is an urgent need to develop new treatments that target brain metastases. Radioimmunotherapy (RIT) is a targeted therapy that uses radiolabeled antibodies against tumor-specific antigens to treat lymphoma patients. However, success of RIT in the therapy of solid tumors has generally been limited due to heterogeneous tumor expression of the target antigens and cross-reactivity with normal cells. In preliminary studies, we have demonstrated that phosphatidylserine (PS) is exposed exclusively on tumor vascular endothelium of brain metastases in mouse models. A novel PS-targeting antibody, PGN635, a fully human monoclonal antibody, was used to target exposed PS in the brain metastases. Our data show that PGN635 binds specifically to tumor vascular endothelial cells in multi-focal brain metastases throughout the whole mouse brain. Vascular endothelium in normal brain tissues is negative. Furthermore, pretreatment with 10Gy of whole brain radiation significantly increased PGN635 binding to tumor vascular endothelial cells and tumor cells by increasing their exposure of PS. Vasculature in irradiated normal brain remained negative for exposed PS.					
15. SUBJECT TERMS- Breast cancer brain metastasis, Phosphatidylserine, Radioimmunotherapy					
16. SECURITY CLASSIFICATION OF:			17. LIMITATION OF ABSTRACT	18. NUMBER OF PAGES	19a. NAME OF RESPONSIBLE PERSON
a. REPORT U	b. ABSTRACT U	c. THIS PAGE U			USAMRMC
			UU	18	19b. TELEPHONE NUMBER (include area code)

Table of Contents

Cover.....	1
SF 298.....	2
Table of Contents	3
Introduction.....	4
Body.....	4
Key Research Accomplishments.....	10
Reportable Outcomes.....	11
Conclusions.....	11
References.....	13
Appendices.....	14

Introduction:

Brain metastasis occurs in ~20% of patients with breast cancer. The prognosis is extremely poor, with a median survival of 4-6 months no matter how aggressive treatment the patients received (1, 2). The incidence of brain metastasis seems to have increased over the past decade. Perhaps even more alarming are the growing numbers of breast cancer patients who die from complications related to brain metastasis, at a time when systemic disease is under good control (3-5). The majority of brain metastases patients exhibit multiple tumors at the time of diagnosis. Even in the event of a solitary metastasis, it is believed that the entire brain can be seeded with many radiographically invisible metastases. Due to the high incidence of multiple brain lesions and the limited leakage of most chemotherapeutics through blood brain barrier (BBB), the standard care for these patients is whole brain radiotherapy (WBRT). WBRT, however, is often associated with neurological complications that preclude sufficient doses delivered to tumor lesions (2, 6). Thus, there is an urgent need to develop new treatment regimens against the devastating disease.

Monoclonal antibody-based therapies, *i.e.*, anti-Her2 trastuzumab, are demonstrating clinical efficacy in treating primary breast cancer (7). However, inability to cross BBB limits their application for treatment of brain metastases. Radioimmunotherapy (RIT), by linking antibodies with radioisotopes, enhances tumor cytotoxicity by directly killing antibody-binding tumor cells or killing neighboring tumor cells by crossfire effect (8, 9). RIT thus offers an opportunity to selectively radiate tumor cells while sparing normal tissues. The high energy β^- emitter, Yttrium-90 (^{90}Y), a FDA approved radiotherapeutic, has been successfully used clinically to treat Non-Hodgkin's lymphomas (10, 11). However, success of RIT in the therapy of solid tumors has generally been limited due to heterogeneous tumor expression of the target antigens and cross-reactivity with normal cells.

Our preliminary studies have found that phosphatidylserine (PS) is exposed extensively on tumor vascular endothelium of brain metastases, but not blood vessels of normal brain in a mouse model of breast cancer brain metastasis (12). A novel PS-targeting, fully human antibody, PGN635, has been applied and showed a great sensitivity and specificity of binding exposed PS in these brain metastases. Furthermore, pretreatment with low dose of whole brain radiation significantly increased PGN635 binding to tumor vascular endothelial cells and tumor cells by increasing their exposure of PS. Given it's specifically for tumor vasculature and the lack of a need to cross the BBB, we propose to apply PGN635 RIT to treat brain metastasis of breast cancer in mouse models. We further hypothesize that RIT in combination with low dose WBRT will not only achieve effective treatment of brain metastases but also minimize the side effects.

Because PS is the same molecule and has the same distribution and regulation in all mammalian species, it is likely that the mouse data will extrapolate to humans. We believe that successful completion of this project will lay a foundation for clinical development of a novel treatment for breast cancer brain metastasis.

Body:

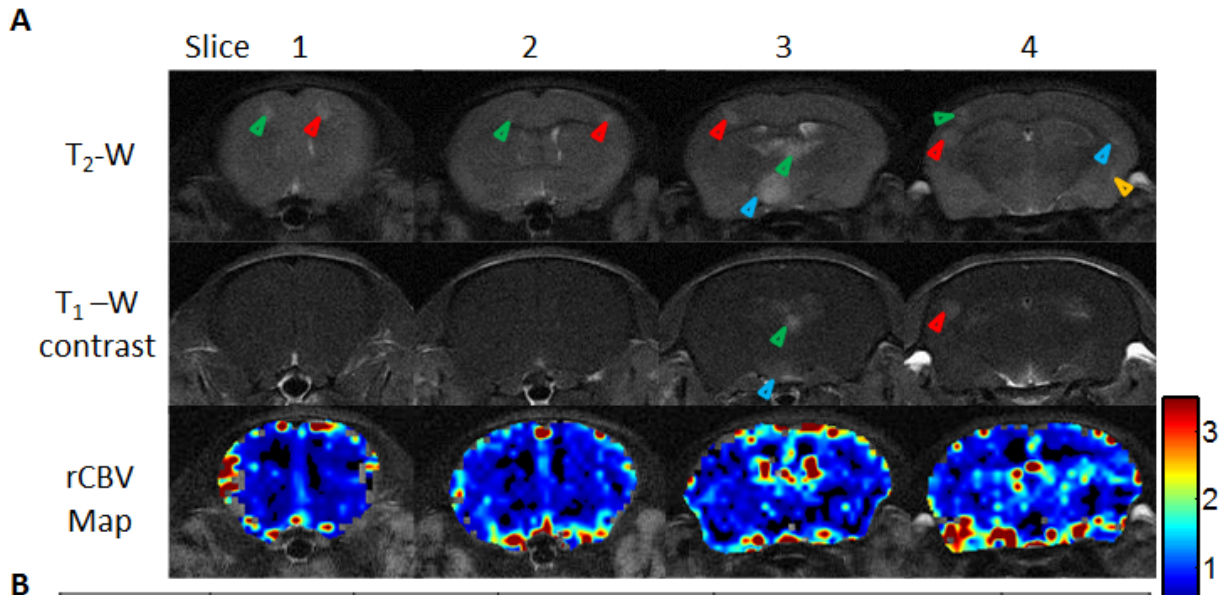
The Statement of Work in this period had two major tasks:

Task 1. To study phosphatidylserine (PS) exposure on tumor vasculature and tumor cells of breast cancer brain metastasis mouse models, and determine if exposed PS is increased by radiation.

a. Establishment of various breast cancer brain metastases mouse models:

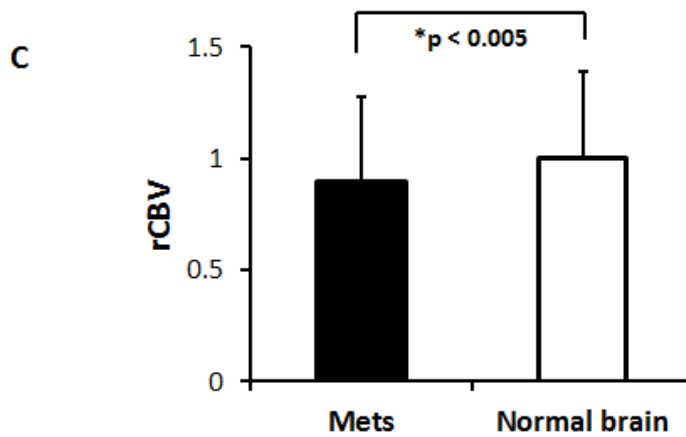
The intracardiac model of Breast cancer brain metastasis has been successfully established by ultrasound-guided left ventricle injection of various breast cancer brain seeking cells, including MDA-MB231Br-EGFP, MCF7Br-Her2 (kindly provided by Drs. Palmieri and Steeg) and syngeneic 4T cells.

b. MRI monitoring of intracranial growth of brain metastasis and vascularity:
 Extensive MRI studies of development of intracranial metastases and their vasculature have been conducted (Fig. 1A-C). Functional MRI measurements of vascular perfusion revealed significantly lower tumor perfusion in metastases as compared to the contralateral normal brain. The observations concur well with histological study of microvessel density (MVD, Fig. 1D-F).



B

	slice 1		slice 2		slice3			slice4			Mean	
Mets	0.72	0.60	1.19	0.45	0.54	1.12	0.68	0.57	1.04	0.83	0.56	0.76±0.26
Contralateral	1.09	1.13	0.58	0.78	0.88	1.61	0.41	0.81	0.97	1.04	1.71	1.00±0.39



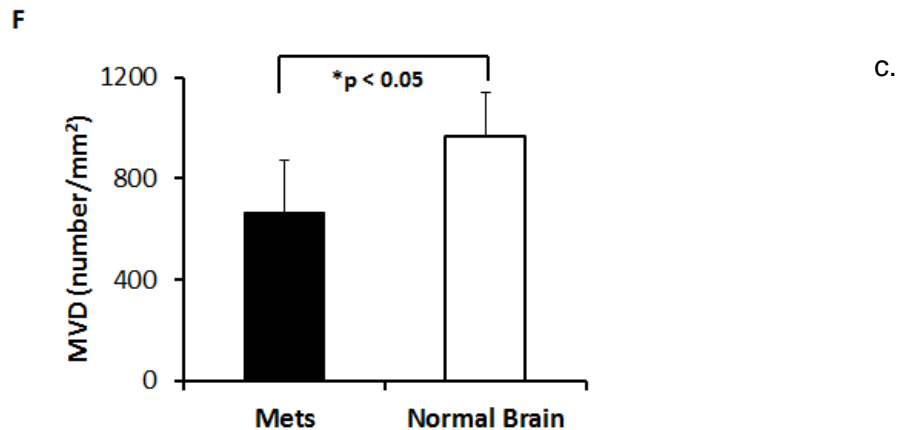
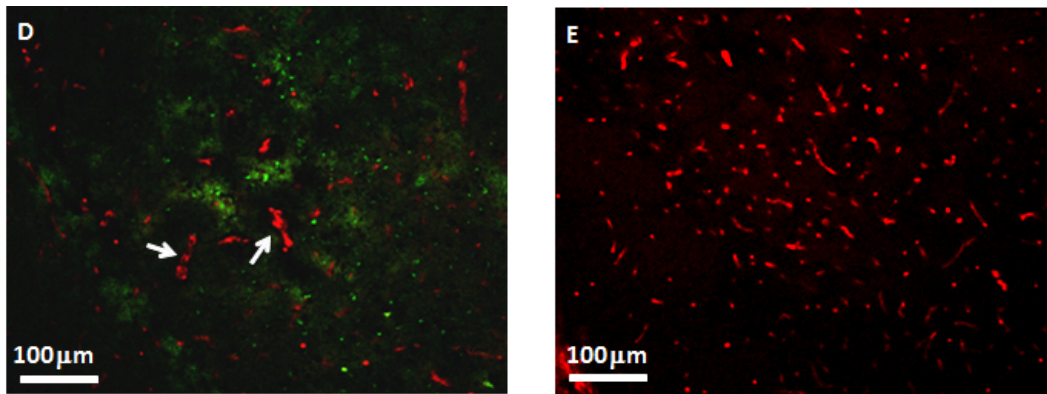


Fig. 1 MRI evaluation of tumor vascularity of brain metastases and correlating with histological studies. **A.** Four weeks after intracardiac injection of ^{231}Br cells, T_2 -weighted MRI revealed multiple high signal intensity lesions (arrowheads) on four consecutive coronal sections of a representative mouse brain. Only a few of the lesions (arrowheads) were enhanced on T_1 -weighted post contrast images, one (blue arrowhead in the MRI section 3) of which showed partial enhancement, indicating intratumoral heterogeneity of BTB disruption. rCBV maps of the four sections were generated and overlaid on the T_2 -weighted images. **B.** The rCBV values of the metastatic lesions and their contralateral normal brain were obtained and summarized in the table. Note the color presented in the table coincides with the color of arrowhead on each of the MR images. Most of metastatic lesions had lower rCBV values than their contralateral counterparts of normal brain. **C.** Statistical analysis of rCBV in a total of 212 lesions of 9 animals obtained from the last follow-up MRI showed significantly lower rCBV of the metastatic tumors with a mean value of 0.89 ± 0.03 (s.e.), compared to the contralateral normal brain (mean = 1.00 ± 0.03 ; $p < 0.005$). **D.** Anti-CD31 staining was performed on a brain section bearing metastases. A cortical lesion ($\sim 600 \mu\text{m}$ in diameter) was depicted with green fluorescence (GFP). Microvessels (red) within the lesion appeared less dense, as compared to abundant fine vessels in the contralateral normal brain tissues (**E**). Some of the tumor vessels were irregular in shape and larger in diameter (arrow). **F.** Quantitative data of MVD showed a significantly lower MVD in brain metastases versus contralateral normal brain (mean = $669 \pm 201/\text{mm}^2$ vs. $965 \pm 177/\text{mm}^2$; $p < 0.05$).

T₁-weighted contrast enhanced MRI was applied to study BTB permeability of brain metastases. A total of 464 metastases were studied, of which 160 (34%) lesions were enhanced on T₁-weighted post contrast images, indicating a locally disrupted BTB (Figs. 2). However, enhancement in some of the metastases was only seen in partial regions of the tumor (Fig. 2), suggesting intratumoral heterogeneity of BTB disruption. Moreover, there was no significant difference in tumor size between permeable and non-permeable metastases ($p = 0.1$, Fig. 2b).

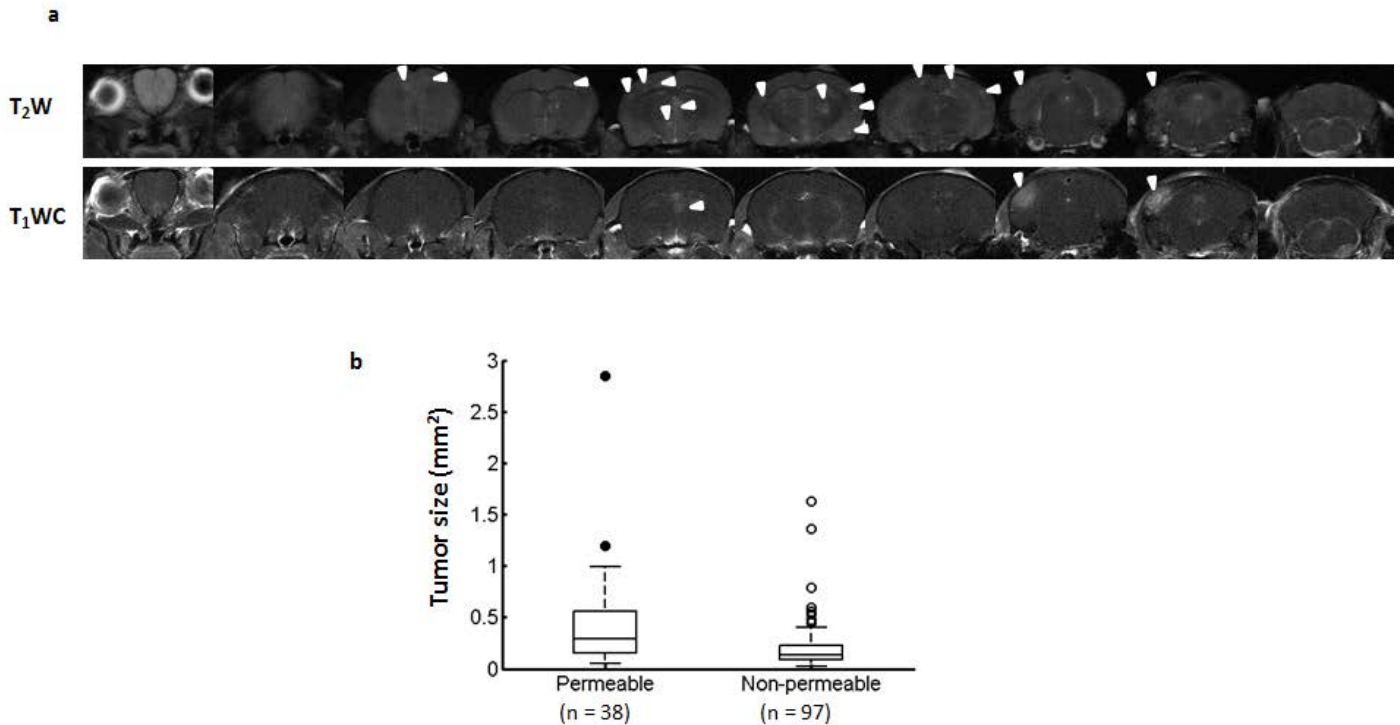


Fig. 2 MRI monitoring of intracranial distribution of brain metastases and permeability of blood-tumor-barrier. a. Ten consecutive MRI coronal sections covering the entire mouse brain were obtained from a representative mouse brain bearing 231-Br metastases. T₂-weighted images revealed hyperintense individual metastases (arrowhead) throughout the entire brain. T₁-weighted post contrast images showed enhancement only in 2 lesions (arrowhead), suggesting a disrupted BTB. **b.** A total of 128 metastases from 6 mice were separated into non-permeable and permeable metastases based on T₁-weighted post contrast images. A plot of permeability versus size indicated that larger metastases tend to be leaky. However, there was no significant difference in tumor size between permeable and non-permeable metastases ($p = 0.1$).

c. Detection and quantification of exposed PS.

PS exposure on vascular endothelium and tumor cells of brain metastases were quantified based on immunohistochemical staining of PGF635 and co-stained with vascular endothelial marker, CD31 (Fig. 3).

Individual brain metastases of MDA-MB231Br can clearly be depicted simply based on PGN635 staining (Fig. 3). Quantitative analysis of PS exposure on vascular endothelial cells of brain metastases revealed $93 \pm 5\%$ of tumor vessels had exposed PS. By contrast, the control antibody, Aurexis showed essentially no staining of blood vessels of brain metastases. The data

suggest that PS is highly specific to tumor vasculature of brain metastases (Fig. 3). Immunohistochemical studies were also conducted on investigating if tumor hypoxia induces PS exposure on vascular endothelial cells. Our data showed that there was no hypoxic regions in individual metastases by pimonidazole staining, indicating other causes than hypoxia may be related to PS exposure.

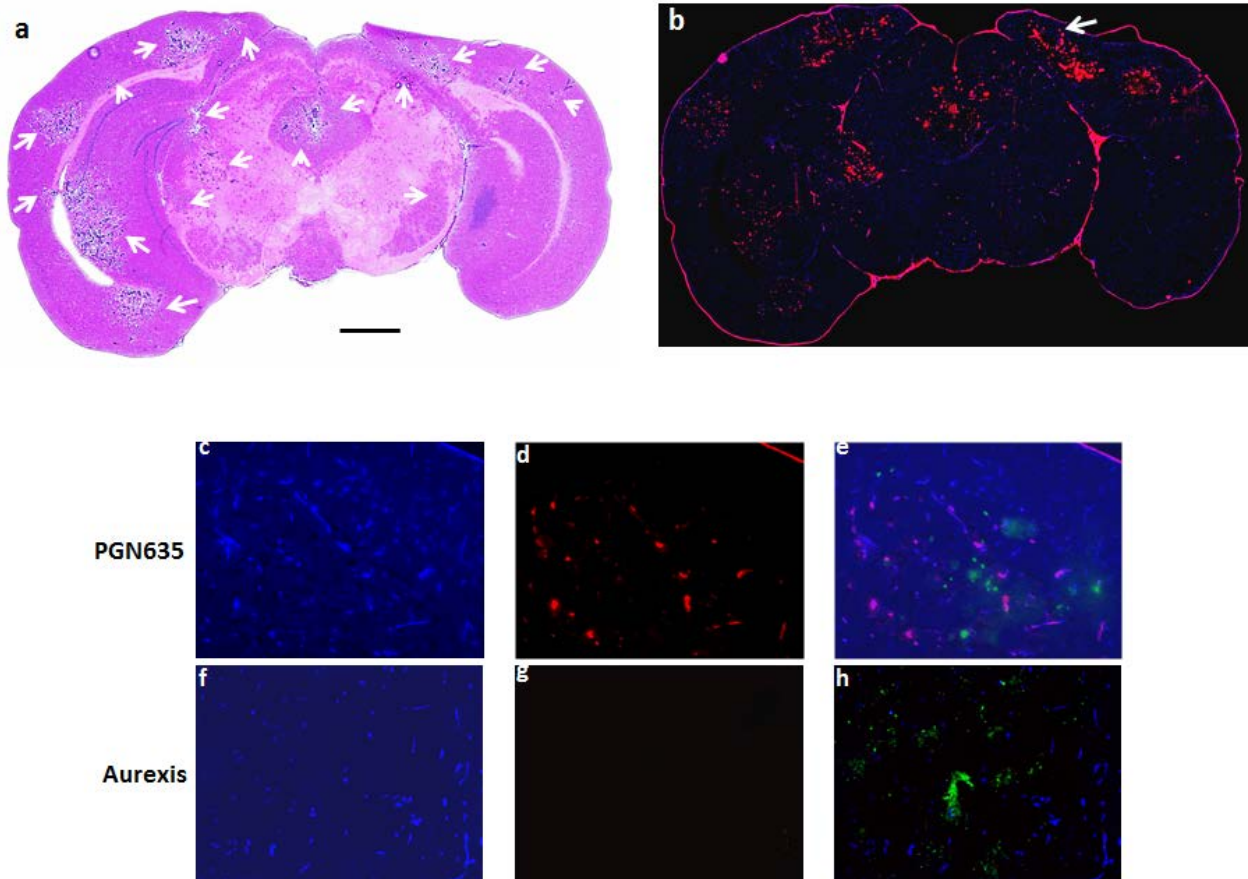


Fig. 3 Staining of PGN635 depicts individual brain metastases. **a.** H&E staining of a representative brain section bearing 231-Br metastases showed multiple lesions. **b.** Immunofluorescent staining on a consecutive section showed that PGN635 (red) localized to individual tumor lesions, even microscopic lesions. Bar=1 mm. **c-e.** A representative region containing positive PGN635 (arrow in **b**) was magnified. The merged image showed that PGN635 (red, **d**) co-localized with almost every CD31-positive tumor vessel (blue, **c**) to give a magenta color (**e**). Vessels in nearby normal brain (containing no GFP) were not stained by PGN635. **f-h.** By contrast, the control antibody, Aurexis showed essentially no staining of blood vessels of brain metastases.

d. Detection and quantification of exposed PS after whole brain radiation.

Irradiation studies with WBRT of a single dose of 10 Gy were undertaken in the brain metastasis-bearing mice. As presented in Fig. 4, a 4T1 brain metastasis was visualized on T2-weighted MRI. A 10 Gy WBRT induced significantly increased PS exposure in not only tumor vascular endothelial cells but also massive tumor cells (Fig. 4).

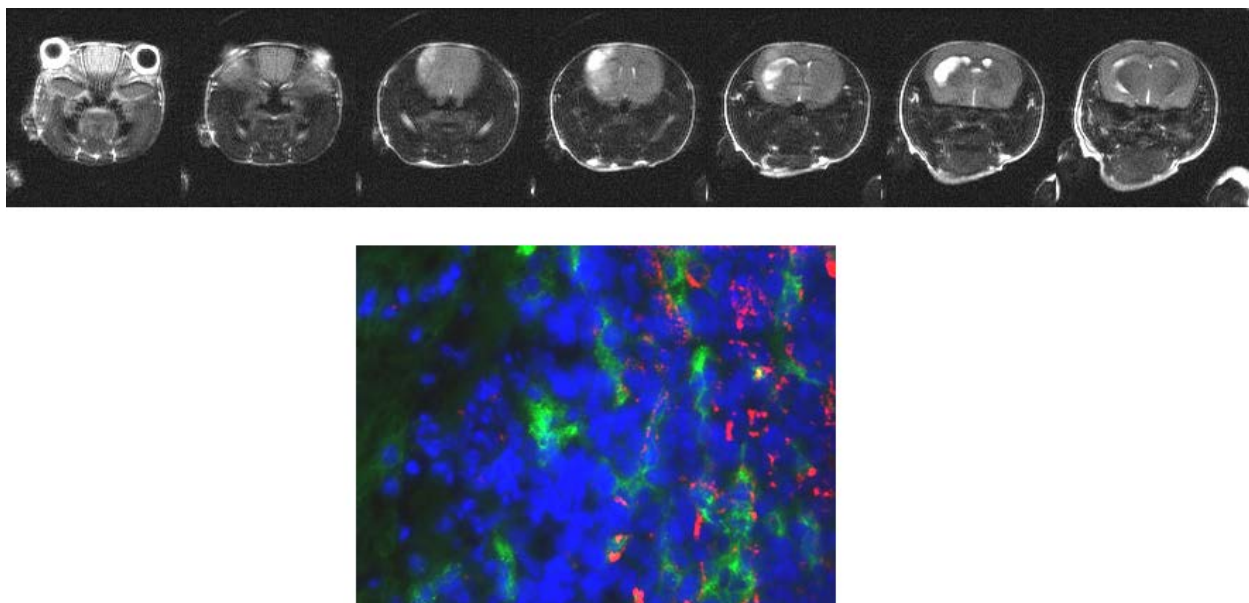


Fig. 4 Enhanced PS exposure after WBRT. Top. T2-weighted MRI clearly revealed a high-signal intensity tumor lesion. **Bottom.** After a single dose of 10 Gy WBRT, immunohistochemical staining was conducted on the tumor specimen with CD31 (green), PGN635 (red) and Dapi (blue). In addition to vascular exposed PS (orange), massive tumor cells were detected with PS exposure.

Task 2. To radiolabel the PS-targeting antibody, mch635, with β^- emitters and evaluate its biodistribution and pharmacokinetics in breast cancer brain metastasis mouse models.

- a. Radiolabel PGN635F(ab')₂
- b. Evaluate stability and binding specificity of the radio-conjugates *in vitro*.
- c. Develop breast cancer brain metastasis with the 4 breast cancer cell lines.
- d. MRI monitoring of intracranial growth of brain metastasis.
- e. *In vivo* studies of biodistribution and dosimetry in healthy mice and in mice bearing brain metastases.

PGN635F(ab')₂ were successfully labeled with I-124 to study its specific targeting of brain metastases and biodistribution. The imaging data in Fig.5 indicated that the radiolabeled PGN635 can serve as a specific imaging probe for sensitive detection of brain metastases in mice.

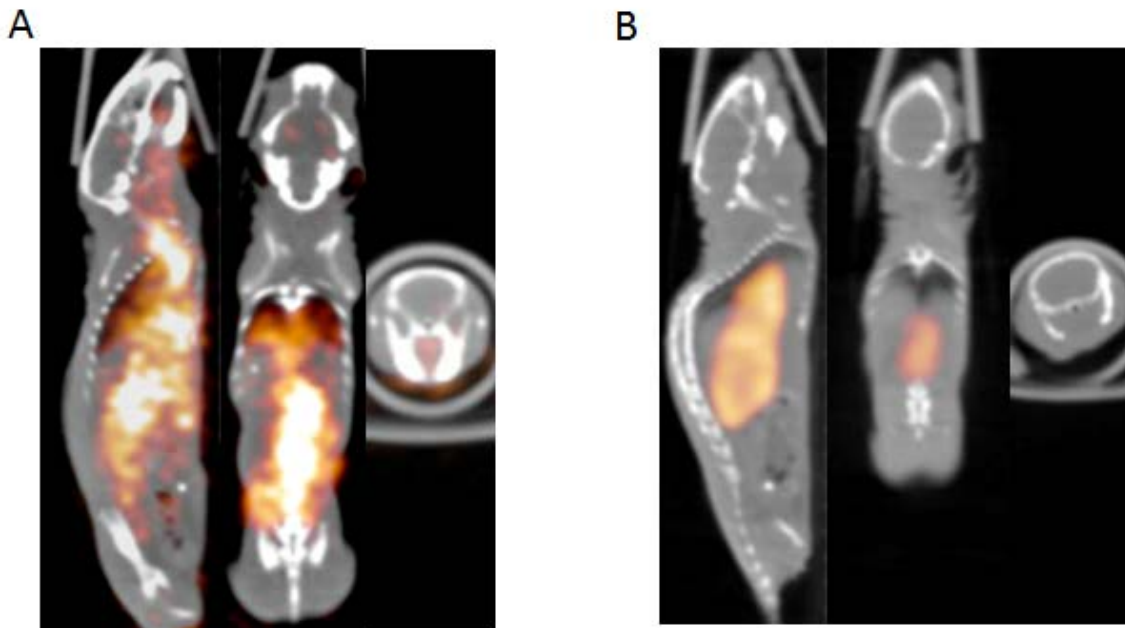


Fig. 5 PS-targeted PET imaging of brain metastases. **A.** A mouse bearing multiple MDA-MB231BR brain metastases was given i.v. ^{124}I -PGN635 $\text{F}(\text{ab}')_2$ ($50\ \mu\text{g} / 50\ \mu\text{Ci}$) via a tail vein. PET/CT images were acquired 48 h. Representative merged images at sagittal, axial and coronal plane showed multiple localized uptake in the mouse brain, indicating the uptake of ^{124}I -PGN635 by the metastatic lesions. By contrast, there was a complete lack of uptake of ^{124}I -PGN635 in a normal control mouse.

Key Research Accomplishments

- Extensive imaging studies of the intracardiac model of breast cancer brain metastasis with various brain-tropic metastatic breast cancer cells including MDA-MB231Br-EGFR, MCF7Br-Her2 and syngeneic 4T1 cells.
- MRI was applied to evaluate vascular perfusion and BTB permeability of brain metastases. Our data showed significantly lower tumor perfusion in brain metastases as compared to the contralateral normal brain, and less than half of brain metastases containing disruptive blood-tumor-barrier (BTB), which correlated well with histological analyses.
- Immunohistochemical studies show PS exposure is specifically located on tumor vascular endothelial cells of brain metastases while the normal vessels surrounding the metastases lack of exposed PS, suggesting that PS can serve as a brain metastasis-specific biomarker.
- Whole brain radiation (WBRT) induced significantly more PS exposure on both tumor vascular endothelial cells and tumor cells of brain metastases.

- **PS-targeting antibody, PGN635F(ab')₂ has been successfully conjugated with radioisotope, enabling in vivo PET imaging for sensitive detection of brain metastases.**

Technique problem

Due to the loss of Dr. Thorpe, the Partner PI and the delay in replacement of Dr. Thorpe with Dr. Brekken, the studies, in particular, Task 2 proposed in this project were significantly delayed. Thus, we requested a 12 month NCE to fulfill the remaining studies.

Reportable Outcomes

Publications:

Peer-reviewed paper:

1. Zhou, H. and **Zhao, D.** Ultrasound imaging-guided intracardiac injection to develop a mouse model of breast cancer brain metastases followed by longitudinal MRI. *J. Vis. Exp.* e51146, 2014. PMID: 24637963.

Manuscript in preparation

1. Zhou, H., Stafford, J.H., Chiguru, S. and **Zhao, D** Targeting phosphatidylserine enables the clear demarcation of brain metastases in mouse models. Manuscript in preparation.

Employment or research opportunity:

The Postdoctoral fellow, Liang Zhang, PhD., has been dedicating on this project.

Conclusion:

During the second year of this project, we continued to perform extensive imaging and correlative histological studies to interrogate brain metastases in mouse models of various brain-tropic breast cancer cell lines. Vascular perfusion and permeability of these metastases were thoroughly assessed by functional MRI. The high sensitivity and specificity of the novel phosphatidylserine-targeting antibody, PGN635 enables individual metastases, even those micrometastases containing intact BTB to be clearly delineated. Non-invasive imaging of mice injected with PGN635 labeled with IRDye 800CW or radioisotope ¹²⁴I allowed clear visualization of individual brain metastases. Given its intravascular localization and the lack of a need to cross the BTB, PS appears to be an excellent marker for the development of imaging and targeted therapeutics for brain metastases. Therapeutic studies are currently undertaken. We are confident that we will complete the proposed studies by the end of NCE period.

References:

1. Chang EL, Lo S. Diagnosis and management of central nervous system metastases from breast cancer. *Oncologist* 2003; 8: 398-410.
2. Gaspar L, Scott C, Rotman M, et al. Recursive partitioning analysis (RPA) of prognostic factors in three Radiation Therapy Oncology Group (RTOG) brain metastases trials. *Int J Radiat Oncol Biol Phys* 1997; 37: 745-51.
3. Subramanian A, Harris A, Piggott K, Shieff C, Bradford R. Metastasis to and from the central nervous system--the 'relatively protected site'. *Lancet Oncol* 2002; 3: 498-507.
4. Begley DJ. Delivery of therapeutic agents to the central nervous system: the problems and the possibilities. *Pharmacol Ther* 2004; 104: 29-45.
5. Doolittle ND, Abrey LE, Bleyer WA, et al. New frontiers in translational research in neuro-oncology and the blood-brain barrier: report of the tenth annual Blood-Brain Barrier Disruption Consortium Meeting. *Clin Cancer Res* 2005; 11: 421-8.
6. Lutterbach J, Bartelt S, Ostertag C. Long-term survival in patients with brain metastases. *J Cancer Res Clin Oncol* 2002; 128: 417-25.
7. Carter P. Improving the efficacy of antibody-based cancer therapies. *Nat Rev Cancer* 2001; 1: 118-29.
8. Ran S, Downes A, Thorpe PE. Increased exposure of anionic phospholipids on the surface of tumor blood vessels. *Cancer Res* 2002; 62: 6132-40.
9. Ran S, Thorpe PE. Phosphatidylserine is a marker of tumor vasculature and a potential target for cancer imaging and therapy. *Int J Radiat Oncol Biol Phys* 2002; 54: 1479-84.
10. Emmanouilides C. Review of Y-ibritumomab tiuxetan as first-line consolidation radio-immunotherapy for B-cell follicular non-Hodgkin's lymphoma. *Cancer Manag Res* 2009; 1: 131-6.
11. Lau WY, Lai EC, Leung TW. Current Role of Selective Internal Irradiation with Yttrium-90 Microspheres in the Management of Hepatocellular Carcinoma: A Systematic Review. *Int J Radiat Oncol Biol Phys*.
12. Zhao D, Zhou, H., Chiguru, s., Slavine, N., Stafford, J.H., Thorpe, P.E. Targeting Phosphatidylserine enables the clear demarcation of brain metastases in mouse models. *Cell Symposium: Hallmarks of Cancer*, 2012; San Francisco, CA; 2012. p. P2.028.

Appendices

Video Article

Ultrasound Imaging-guided Intracardiac Injection to Develop a Mouse Model of Breast Cancer Brain Metastases Followed by Longitudinal MRI

Heling Zhou¹, Dawen Zhao¹¹Radiology, University of Texas Southwestern Medical CenterCorrespondence to: Dawen Zhao at Dawen.Zhao@utsouthwestern.eduURL: <http://www.jove.com/video/51146>DOI: [doi:10.3791/51146](https://doi.org/10.3791/51146)

Keywords: Medicine, Issue 85, breast cancer brain metastasis, intracardiac injection, ultrasound imaging, MRI, MDA-MB231/Br-GFP cells

Date Published: 3/6/2014

Citation: Zhou, H., Zhao, D. Ultrasound Imaging-guided Intracardiac Injection to Develop a Mouse Model of Breast Cancer Brain Metastases Followed by Longitudinal MRI. *J. Vis. Exp.* (85), e51146, doi:10.3791/51146 (2014).

Abstract

Breast cancer brain metastasis, occurring in 30% of breast cancer patients at stage IV, is associated with high mortality. The median survival is only 6 months. It is critical to have suitable animal models to mimic the hemodynamic spread of the metastatic cells in the clinical scenario. Here, we are introducing the use of small animal ultrasound imaging to guide an accurate injection of brain tropical breast cancer cells into the left ventricle of athymic nude mice. Longitudinal MRI is used to assessing intracranial initiation and growth of brain metastases. Ultrasound-guided intracardiac injection ensures not only an accurate injection and hereby a higher successful rate but also significantly decreased mortality rate, as compared to our previous manual procedure. *In vivo* high resolution MRI allows the visualization of hyperintense multifocal lesions, as small as 310 μm in diameter on T₂-weighted images at 3 weeks post injection. Follow-up MRI reveals intracranial tumor growth and increased number of metastases that distribute throughout the whole brain.

Video Link

The video component of this article can be found at <http://www.jove.com/video/51146/>

Introduction

Brain metastasis is the most common intracranial malignancy in adults. The prognosis is extremely poor, with a median survival of 4-6 months even with aggressive treatment. Breast cancer is one of the three major primary cancers with a high morbidity of brain metastasis¹⁻³. Several brain-tropic breast cancer lines are capable of developing brain metastases after intracardiac or intracarotid injection⁴. Direct injection of tumor cells into the left ventricle can bypass the lung capillary bed and thus increase the incidence of forming brain metastases while minimizing visceral metastases. The MDA-MB231Br line is one of the most widely used human breast cancer lines to develop brain metastasis in rodent models^{5,6}.

Like many other studies^{4,7}, we have performed a manual procedure of intracardiac injection in our previous studies. However, only 50% successful rate was obtained with the manual injection and a fraction of mice died from the repeated invasive procedures if prior trials failed. Here, we are introducing the use of an imaging-guided procedure to secure the injection of brain-seeking breast cancer cells into the left ventricle of athymic mice. Longitudinal high resolution MRI is applied to follow intracranial development of brain metastases.

Protocol

All animal procedures were approved by the Institutional Animal Care and Use Committee of University of Texas Southwestern Medical Center.

1. Preparation of the MDA-MB231/Br-GFP Cells

1. Retrieve and culture the MDA-MB231/Br-GFP cells (kindly provided by Drs. Palmieri and Steeg, NCI) in DMEM medium containing 10% FBS, 1% glutamine and 1% penicillin/streptomycin.
2. Observe the condition of the cells and color of medium, and replace medium every 2-3 days.
3. Trypsinize and collect the cells when 80% confluence is reached as outlined in steps 1.3.1-1.3.5:
 1. Remove the old medium completely and add 5 ml PBS (1x) to wash the cells gently. Remove the PBS from the dish.
 2. Add 1.5 ml Trypsin in the dish; tilt the dish gently to ensure all the cells are covered by Trypsin. Put the dish back to the cell incubator and keep it at 37 °C for 1 min.
 3. Take the dish out of incubator and observe the cells under optical microscope to ensure the cells detach from the dish.
 4. Add 3 ml medium to stop the effect of trypsin. Collect the cell mixture in a centrifuge tube. Centrifuge the mixture at 2,000 rpm for 5 min.
 5. Remove the medium carefully and resuspend the cells in 5 ml serum free medium until homogenous.

4. Count appropriate number of cells and resuspend them in serum free DMEM medium with a final concentration of 1.75×10^5 cells in 100 μ l volume.
 1. Take 50 μ l cell mixture and add 50 μ l Trypan Blue. After mixing, take 10 μ l mixture and carefully add to the cell counting slide. Use multiple samples to ensure accurate cell number estimation.
 2. Stick in the cell counting slide, one end at a time and the cell counter starts counting automatically. Take average of all the counting results and calculate the total cell number.
 3. Centrifuge the cells again and resuspend them in the appropriate volume of serum free medium to result in the final concentration of 1.75×10^5 cells/100 μ l volume.
5. Place cells on ice prior to intracardiac injection.

2. Ultrasound Imaging-guided Intracardiac Injection

1. Use female nude mice (BALB/c nu/nu) between 6-8 weeks old.
2. Log in the imaging system. Initialize the transducer 704 (40 MHz).
3. Start a new study and fill in the information.
4. Anesthetize (3% isoflurane/100% O₂ in an induction chamber) and maintain the animals with isoflurane (2%) in 100% O₂ (1 dm³/min) during the whole procedure via a nose cone. Anesthesia is confirmed when no withdrawal reflex is observed with toe pinch.
5. Set the temperature of the imaging table to 37 °C. Tape the anesthetized mouse to the heated imaging table in supine position.
6. Keep the ultrasound gel at 37 °C prior to imaging. Apply the gel to the chest of the mouse.
7. Mount the transducer in the holder. Lower the transducer till the desired imaging depth is reached. Move the stage until the left ventricle is identified with the ascending aorta as the landmark (**Figure 1A**). Lock the stage when a clear view of left ventricle is visualized.
8. Draw 100 μ l of cell mixture into a 1 ml syringe with a 22 G needle. Place and fix the syringe on the syringe mount.
9. Move the syringe forward towards the mouse chest and carefully move it side to side until the needle tip is in the imaging field of view (before entering the mouse).
10. Adjust the needle height and angle to aim down the left ventricle.
11. Penetrate the syringe needle into intercoastal space promptly through skin and muscle layers into the left ventricle under the guidance of ultrasound imaging.

An indication of successful insertion of the needle into the left ventricle is the reflux of fresh arterial blood (pink color in contrast to dark red venous blood) into the syringe

12. Inject the cell mixture slowly (**Figure 1B**).
13. Upon completion, withdraw the needle, lift up the transducer, clean the ultrasound gel with dampened gauze and remove tape.
14. Prepare a clean cage with a preheated pad.
15. Place the animal on the pad and observe the animal till full recovery.
16. Monitor the behavior of the animal every 24 hr for two days.
17. General conditions and neurologic signs of complications in experimental mice are routinely monitored.

3. MRI Monitoring of Intracranial Tumor Development

1. Use a 9.4 Tesla magnet to monitor intracranial development of brain metastases.
2. Initiate MRI two weeks after tumor implantation and repeat once a week for up to three weeks.
3. Sedate the animals with 3% isoflurane and maintain them under general anesthesia (1.5% isoflurane).
4. Monitor and maintain the animal body temperature and respiration constant throughout the experiment.
5. High resolution multislice (14 slices with 1 mm thick, no gap) T₁- and T₂-weighted coronal images, covering the region from the frontal lobe to the posterior fossa, are acquired with the following parameters: T₁-weighted images: spin echo multiple slice (SEMS), TR/TE = 400 msec/20 msec, matrix: 256 x 256, FOV 20 x 20 mm, in plane resolution: 78 x 78 μ m². T₂-weighted images: fast spin echo multiple slice (FSEMS) sequences, TR/TE = 2500 msec/48 msec, 8 echo trains, matrix: 256 x 256, FOV 20 x 20 mm, in plane resolution: 78 x 78 μ m^{28,9}.

Tumor lesions appear brighter than normal brain tissues on T₂-weighted images.

6. Tumor size is determined on T₂-weighted images by manually outlining the enhancing portion of the mass on each image by using MATLAB programs written by us⁸.

Given most of the tumor diameters are smaller than the slice thickness (1 mm), the tumor size is presented as in plane area rather than the volume.

4. H&E Staining Confirming the Metastases

1. Sacrifice the mice immediately after the last MR scan, dissect the tumor-bearing brains and embed it in O.C.T medium and frozen in -80 °C.
2. Section a series of 10 μ m-thick coronal brain specimens with cryostat.
3. Perform H&E staining on the brain sections.

Representative Results

With the high spatial resolution of MRI (78 μm in plane resolution), hyperintense lesions can be identified as small as 310 μm in diameter (**Figure 2**). Since the metastases in this study are very small and development of necrosis and edema is minimal, the hyperintense lesion on T_2 -weighted images truly represented the tumor mass.

Longitudinal MRI studies allow *in vivo* noninvasive evaluation of tumor growth. As shown in **Figure 3**, the high resolution MRI was able to detect several small lesions 3 weeks after intracardiac injection (**Figure 3A**). On week 4, the lesions that were seen in the previous scan all became larger; more new lesions appeared on T_2 -weighted images (**Figure 3B**).

H&E staining revealed either diffuse or cluster type metastatic lesions (**Figure 4**). Enlarged vessels were often seen around the tumor, indicating nonsprouting angiogenesis (**Figure 4D**).

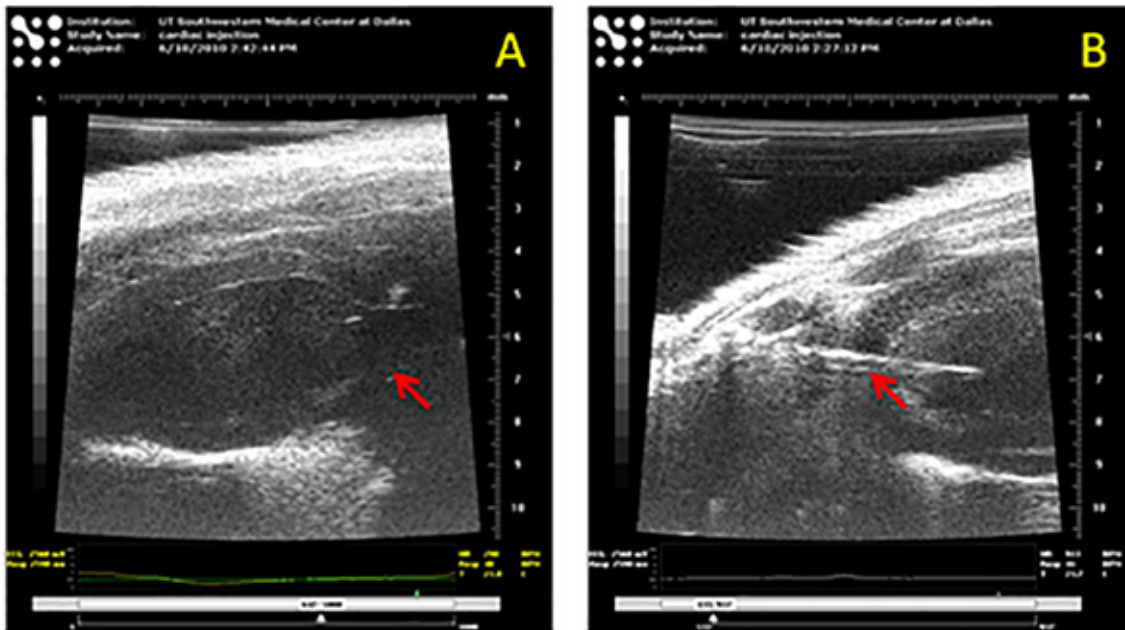


Figure 1. Ultrasound-guided intracardiac injection. (A) Identification of the ascending aorta (arrow) as the landmark of left ventricle of the mouse heart. (B) A needle (arrow) insertion into the left ventricle to inject the tumor cells. [Click here to view larger image.](#)

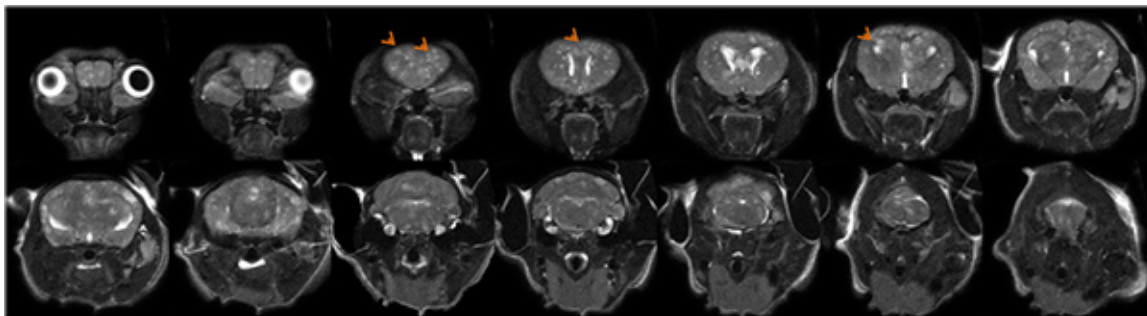


Figure 2. High resolution T_2 -weighted images of breast cancer brain metastases. Fourteen consecutive MRI slices of a representative mouse brain, acquired four weeks after intracardiac injection, clearly revealed the multifocal metastases distributing through the whole mouse brain, from olfactory bulb to pontine and medulla. [Click here to view larger image.](#)

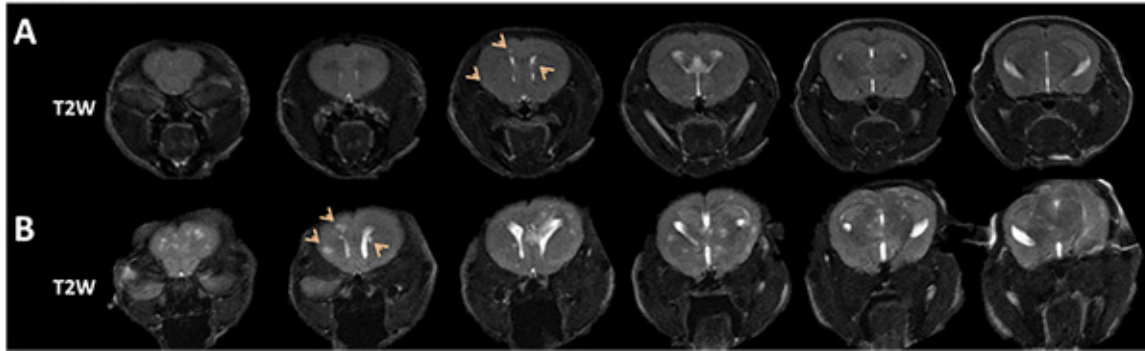


Figure 3. Longitudinal MRI of development of brain metastases. **A.** Six consecutive coronal MRI sections at week 3 identified multiple lesions with hyper-intensity on T_2 -weighted images. **B.** An increased number of lesions appeared on the images at week 4, and those lesions seen on week 3 became larger. [Click here to view larger image.](#)

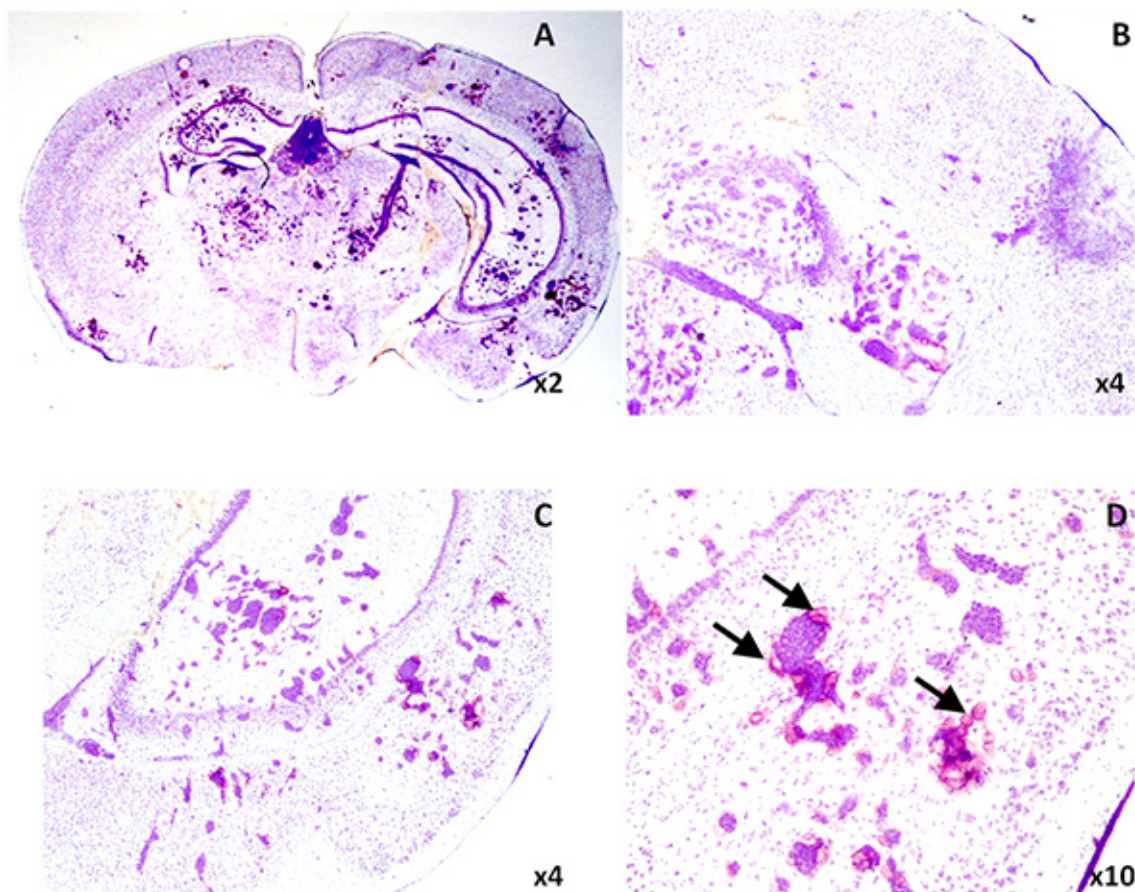


Figure 4. Microscopic lesions were observed on H&E staining. **A.** A whole mount coronal section depicted multiple lesions. **B-D.** Higher magnification images showed either diffuse or cluster type lesions (**B** and **C**). Enlarged vessels were seen around the tumor. [Click here to view larger image.](#)

Discussion

In the present study, we have demonstrated that ultrasound imaging-guided left ventricular injection ensures the accuracy so that every animal in this study developed brain metastases and no animal death was observed. The beauty of image-guided injection is that the path of needle penetration of skin and finally into the left ventricle can be monitored and adjusted under image, which is distinct from the manual procedure requiring strict anatomic landmarks to follow.

Current understandings of intracranial development of brain metastases are largely based on histological studies on animal models^{4,10}. However, histological studies normally require a large number of mice that are killed at different time points after tumor implantation. More importantly, information about temporal development in individual lesions is lacking from histological studies.

In vivo imaging promises greater efficiency since each animal serves as its own control and multiple time points can be examined sequentially^{7,11}. High resolution T₂-weighted images enable the detection of multifocal tumor initiation at very early stage (lesions with diameter as small as 310 μm are visible). Longitudinal MRI allows individual brain metastases to be examined over time. Moreover, *in vivo* noninvasive MRI will be particularly valuable in longitudinal study of therapeutic response, e.g. whole brain radiation.

Formation of multifocal brain metastases is the characteristics of the MDA-MB231Br model. Besides the MDA-MB231/Br-GFP cell line we showed in the present study, the parental clone MDA-MB231/Br and MDA-MB231/Br-luc also exhibit similar metastatic lesions. In contrast, several other brain-seeking lines such as MCF-7Br and 4T1 have been shown to develop a solitary metastasis after intracardiac injection¹². Both of the models, mirroring clinical counterparts, are useful animal models of brain metastasis. However, in addition to brain metastases, visceral metastases, such as lung and bone metastases are often observed in this model. Establishment of animal models that develop brain metastases exclusively will be critical, in particular, for evaluation of treatment response.

In conclusion, we have demonstrated the usefulness of imaging-guided intracardiac injection to establish a brain metastasis mouse model and the high resolution MRI to assess intracranial development of multifocal metastases in a mouse model.

Disclosures

No conflicts of interest declared.

Acknowledgements

We are grateful to Drs. Diane Palmieri and Patricia Steeg of NCI for providing us MDA-MB231Br cells. We thank Dr. Ralph Mason, Mr. Jason Reneau and Ms. Ramona Lopes for technical and collegial support. This work was supported in part by the DOD IDEA Awards W81XWH-08-1-0583 and W81XWH-12-1-0317. MRI experiments were performed in the Advanced Imaging Research Center, an NIH BTRP # P41-RR02584 facility, and ultrasound-guided intracardiac injection was performed with VisualSonics Vevo 770 under 1S10RR02564801.

References

- Schouten, L. J. *et al.* Incidence of brain metastases in a cohort of patients with carcinoma of the breast, colon, kidney, and lung and melanoma. *Cancer*. **94**, 2698-2705 (2002).
- Lin, N. U. *et al.* CNS metastases in breast cancer. *J. Clin. Oncol.* **22**, 3608-3617, doi:10.1200/JCO.2004.01.175 22/17/3608 [pii] (2004).
- Eichler, A. F. *et al.* The biology of brain metastases-translation to new therapies. *Nat. Rev. Clin. Oncol.* doi:nrclinonc.2011.58 [pii] 10.1038/nrclinonc.2011.58 (2011).
- Lockman, P. R. *et al.* Heterogeneous blood-tumor barrier permeability determines drug efficacy in experimental brain metastases of breast cancer. *Clin. Cancer Res.* **16**, 5664-5678, doi:1078-0432.CCR-10-1564 [pii] 10.1158/1078-0432.CCR-10-1564 (2010).
- Yoneda, T. *et al.* A bone-seeking clone exhibits different biological properties from the MDA-MB-231 parental human breast cancer cells and a brain-seeking clone *in vivo* and *in vitro*. *J. Bone Miner. Res.* **16**, 1486-1495 (2001).
- Palmieri, D. *et al.* Her-2 overexpression increases the metastatic outgrowth of breast cancer cells in the brain. *Cancer Res.* **67**, 4190-4198, doi:67/9/4190 [pii] 10.1158/0008-5472.CAN-06-3316 (2007).
- Percy, D. B. *et al.* *In vivo* characterization of changing blood-tumor barrier permeability in a mouse model of breast cancer metastasis: a complementary magnetic resonance imaging approach. *Invest. Radiol.* **46**, 718-725, doi:10.1097/RLI.0b013e318226c427 (2011).
- Zhou, H. *et al.* Longitudinal MRI evaluation of intracranial development and vascular characteristics of breast cancer brain metastases in a mouse model. *PLoS One*. **8** e62238, doi:10.1371/journal.pone.0062238 (2013).
- Zhou, H. *et al.* Dynamic near-infrared optical imaging of 2-deoxyglucose uptake by intracranial glioma of athymic mice. *PLoS One*. **4**, e8051, doi:10.1371/journal.pone.0008051 (2009).
- Zhang, R. D. *et al.* Differential permeability of the blood-brain barrier in experimental brain metastases produced by human neoplasms implanted into nude mice. *Am. J. Pathol.* **141**, 1115-1124 (1992).
- Mason, R. P. *et al.* Tumor oximetry: comparison of 19F MR EPI and electrodes. *Adv. Exp. Med. Biol.* **530**, 19-27 (2003).
- Gril, B. *et al.* Pazopanib reveals a role for tumor cell B-Raf in the prevention of HER2+ breast cancer brain metastasis. *Clin. Cancer Res.* **17**, 142-153, doi:1078-0432.CCR-10-1603 [pii] 10.1158/1078-0432.CCR-10-1603 (2010).